


Underestimated ecosystem carbon turnover time and sequestration under the steady state assumption: A perspective from long-term data assimilation

Rong Ge^{1,2}  | Honglin He^{1,3} | Xiaoli Ren¹ | Li Zhang^{1,3} | Guirui Yu^{1,3} | T. Luke Smallman⁴ | Tao Zhou⁵ | Shi-Yong Yu⁶ | Yiqi Luo⁷ | Zongqiang Xie⁸ | Silong Wang⁹ | Huimin Wang¹ | Guoyi Zhou¹⁰  | Qibin Zhang⁸  | Anzhi Wang⁹ | Zexin Fan¹¹ | Yiping Zhang¹¹ | Weijun Shen¹⁰  | Huajun Yin¹² | Luxiang Lin¹¹

¹Key Laboratory of Ecosystem Network Observation and Modeling, Institute of Geographic Sciences and Natural Resources Research, Chinese Academy of Sciences, Beijing, China

²University of Chinese Academy of Sciences, Beijing, China

³College of Resources and Environment, University of Chinese Academy of Sciences, Beijing, China

⁴School of GeoSciences, University of Edinburgh, Edinburgh, UK

⁵State Key Laboratory of Earth Surface Processes and Resource Ecology, Beijing Normal University, Beijing, China

⁶Large Lakes Observatory, University of Minnesota Duluth, Duluth, Minnesota

⁷Center for Ecosystem Science and Society (EcoSS) and Department of Biological Sciences, Northern Arizona University, Flagstaff, Arizona

⁸Institute of Botany, Chinese Academy of Sciences, Beijing, China

⁹Institute of Applied Ecology, Chinese Academy of Sciences, Shenyang, China

¹⁰South China Botanical Garden, Chinese Academy of Sciences, Guangzhou, China

¹¹Key Laboratory of Tropical Forest Ecology, Xishuangbanna Tropical Botanical Garden, Chinese Academy of Sciences, Mengla, China

¹²Chengdu Institute of Biology, Chinese Academy of Sciences, Chengdu, China

Correspondence

Honglin He and Xiaoli Ren, Key Laboratory of Ecosystem Network Observation and Modeling, Institute of Geographic Sciences and Natural Resources Research, Chinese Academy of Sciences, Beijing, China.
Emails: hehl@igsnr.ac.cn and renxl@igsnr.ac.cn

Funding information

National Key Research and Development Program of China, Grant/Award Number: 2016YFC0500204; Strategic Priority Research Program of the Chinese Academy of Sciences, Grant/Award Number: XDA19020301; National Natural Science Foundation of China, Grant/Award Number: 41571424, 31700417

Abstract

It is critical to accurately estimate carbon (C) turnover time as it dominates the uncertainty in ecosystem C sinks and their response to future climate change. In the absence of direct observations of ecosystem C losses, C turnover times are commonly estimated under the steady state assumption (SSA), which has been applied across a large range of temporal and spatial scales including many at which the validity of the assumption is likely to be violated. However, the errors associated with improperly applying SSA to estimate C turnover time and its covariance with climate as well as ecosystem C sequestrations have yet to be fully quantified. Here, we developed a novel model-data fusion framework and systematically analyzed the SSA-induced biases using time-series data collected from 10 permanent forest plots in the eastern China monsoon region. The results showed that (a) the SSA significantly underestimated mean turnover times (MTTs) by 29%, thereby leading to a 4.83-fold underestimation of the net ecosystem productivity (NEP) in these forest ecosystems, a major C sink globally; (b) the SSA-induced bias in MTT and NEP correlates negatively with forest age, which provides a significant caveat for applying the SSA to young-aged ecosystems; and (c) the sensitivity of MTT to temperature

and precipitation was 22% and 42% lower, respectively, under the SSA. Thus, under the expected climate change, spatiotemporal changes in MTT are likely to be underestimated, thereby resulting in large errors in the variability of predicted global NEP. With the development of observation technology and the accumulation of spatiotemporal data, we suggest estimating MTTs at the disequilibrium state via long-term data assimilation, thereby effectively reducing the uncertainty in ecosystem C sequestration estimations and providing a better understanding of regional or global C cycle dynamics and C-climate feedback.

KEYWORDS

carbon sequestration, climate sensitivity, non-steady state, steady state, turnover time

1 | INTRODUCTION

The terrestrial carbon (C) cycle is among the largest uncertainties affecting global C-climate feedback (Le Quéré et al., 2018). Ecosystem C input (gross primary productivity, GPP) and C mean turnover time (MTT) are two key factors in determining the C sequestration capacity of terrestrial ecosystems (Luo et al., 2017; Xia, Luo, Wang, & Hararuk, 2013). Terrestrial GPP has been well studied and exhibits a relatively strong convergence in global modeling studies (Anav et al., 2013), whereas the C turnover time has become the dominant uncertainty in terrestrial ecosystem C sequestration and its response to climate change (Carvalhais et al., 2014; Friend et al., 2014; He et al., 2016). Therefore, accurately quantifying the ecosystem MTT and its relationship with climate is crucial for understanding the present and future C budget dynamics in terrestrial ecosystems.

Ecosystem MTT refers to the average time required for atmospheric CO₂ to enter the ecosystem via plant photosynthesis and return to the atmosphere via C loss pathways, such as ecosystem respiration (RE) and fire (Barrett, 2002). As the current understanding of these C cycle processes is mainly based on first-order kinetics (Manzoni & Porporato, 2009), MTT is commonly defined as the ratio of the C pool to the flux (Bolin & Rodhe, 1973; Friedlingstein et al., 2006; Koven et al., 2015). Therefore, the flux used for MTT estimation (i.e., influx or efflux), the state of C pools, as well as the C allocation and turnover rates that control the C flow in various pools, are all key states and processes that collectively determine for the overall ecosystem turnover time (Sitch et al., 2003; Trumbore, 2006).

Currently, MTT estimations are mainly based on two assumptions, the steady state assumption (SSA) and the non-SSA (NSSA), with each corresponding to specific ecological principles and applicable conditions. Without changes in external driving forces, such as disturbances and climate change, the internal processes of an ecosystem will gradually drive the ecosystem C cycle toward equilibrium (Luo & Weng, 2011), at which C influx equals efflux, C pools are stabilized, and the long-term net ecosystem C exchange becomes zero (i.e., $\overline{\Delta C} = 0$); therefore, the MTT under the SSA can be defined as "stock/influx" (Rodhe, 1978). When ecosystems are subject to natural (e.g., insect outbreaks and fire) and anthropogenic (e.g., land-use change)

disturbances as well as global changes (e.g., increasing atmospheric CO₂, climate warming, and nitrogen deposition), ecosystem C cycling processes become destabilized (Bellassen et al., 2011; Luo & Weng, 2011). Therefore, C pools in ecosystems vary dynamically over time (i.e., $dC/dt \neq 0$), the C influx is not equal to the C efflux, and the MTT under the NSSA should be defined as "stock/efflux" (Schwartz, 1979).

An exact equilibrium is almost impossible to observe in reality; but when the relative difference between input and output is negligible, it is justified and valid to apply SSA (Odum, 1966), usually occurring at large or coarse spatial scales where sufficient variation in the sink/source distribution could balance the gross influx and efflux, or occurring at long-time scales where the effects of transient changes in climate or atmospheric CO₂ could be ignored. Specifically, at the global or continental scale near steady state, the more readily obtained influx can be used to estimate MTT instead of the efflux (Carvalhais et al., 2014; Yan, Luo, Zhou, & Chen, 2014). In addition, key process parameters, such as the allocation and turnover rates, can be optimized and then incorporated into an analytical expression under the SSA to quantify the spatial patterns of ecosystem MTT (e.g., Barrett, 2002; Xia et al., 2013). Furthermore, the state of C pools in global models can be initialized via the spin-up process by iterating from hundred to thousand years in preindustrial period until equilibrium (Taylor, Stouffer, & Meehl, 2012), which determines the C pool size used in the analysis of MTT (Exbrayat, Pitman, & Abramowitz, 2014; Koven et al., 2015; Todd-Brown et al., 2013).

In addition to these aforementioned applications, the SSA has also been widely invoked in MTT research over a considerable range of temporal and spatial scales (e.g., Galbraith et al., 2013; Thurner et al., 2016; Wang et al., 2018; Zhou & Luo, 2008), over which non-steady behavior may exist. This appears to be an imperative choice in the absence of direct measurement of C effluxes, such as heterotrophic respiration, or current or past-historical ecosystem states for constraining the dynamic ecosystem C cycle processes. Specifically, at the regional scale with considerable C sinks, (a) the MTTs are still obtained based on influx, which is much higher than efflux, for example, in the forest ecosystems in eastern China (Wang et al., 2018) and the tropics (Galbraith et al., 2013) that have been shown

to be major C sinks globally (Pan et al., 2011; Piao et al., 2009; Yu et al., 2014); (b) C turnover rates and allocation coefficients are still retrieved under the SSA but further used in a transient simulation of the regional MTT and net ecosystem productivity (NEP) (Zhou & Luo, 2008; Zhou, Shi, Jia, Li, & Luo, 2010; Zhou, Shi, Jia, & Luo, 2013); (c) as global C models have been developed to fine spatial scales, the SSA is also widely used for C pool state initialization at local scales with dynamic C sources or sinks (e.g., young-aged forests) (Carvalhais et al., 2008, 2010; Huang et al., 2011; Law, Thornton, Irvine, Anthoni, & Van, 2001; Morales et al., 2005). Previous studies have reported the uncertainty in C pool states and C cycle parameters induced by the SSA (e.g., Carvalhais et al., 2008, 2010), which may further affect the validity of MTT estimation via the "stock/flux" approach. Therefore, a better understanding of the mismatch between the ideal SSA and realistic disequilibrium state in C turnover time estimation is needed and the effect of such inconsistencies on C sequestration should be determined.

With the development of observational technology and the accumulation of multiple and time-series C cycle datasets over the past decade, our understanding of terrestrial C dynamics has improved; accordingly, C effluxes can be better constrained to return to the definition of MTT at the realistic disequilibrium state (e.g., Bloom, Exbrayat, Ir, Feng, & Williams, 2016). On this basis, researchers have attempted to develop the model-data fusion (MDF) method to estimate ecosystem MTT under the NSSA, which integrates the process-based model and observational data to estimate these C cycle dynamics in better agreement with the actual disequilibrium state (Bloom et al., 2016; Luo et al., 2003; Xu, White, Hui, & Luo, 2006; Zhang, Luo, Yu, & Zhang, 2010; Zhou, Shi, et al., 2013). Moreover, the uncertainty in allocation and turnover parameters as well as C pool states have largely been reduced based on the time-series observations under the NSSA, thereby significantly enhancing the model's ability to predict MTT and NEP (Safta et al., 2015; Smallman, Exbrayat, Mencuccini, Bloom, & Williams, 2017).

Regardless, a detailed comparative analysis of ecosystem MTT estimations under the NSSA and SSA has not been conducted based on multi-source and long-term continuous observational data. In this study, we systematically examined differences in ecosystem C cycle states and processes estimated under the two assumptions as well as the underlying mechanisms within a robust analytical framework, using large amounts of long-term continuous observational soil, biology, and climate data for 10 typical forest ecosystems from the Chinese Ecosystem Research Network (CERN) that represent the East Asian monsoon region, a large C sink accounting for 8% of the global forest NEP (Yu et al., 2014). Our analysis mainly focuses on the mismatch between the two assumptions with regard to (a) the magnitude and spatial pattern of the ecosystem MTT, (b) the relationship between the ecosystem MTT and climate, and (c) the ecosystem C sink in these forest ecosystems. These quantitative comparisons using the proposed framework could provide a reference for future MTT research in terms of SSA/NSSA method selection and facilitate an awareness of the corresponding uncertainty.

2 | MATERIALS AND METHODS

2.1 | Site description

The eastern China monsoon region covers tropical, subtropical, warm temperate, and temperate climate zones from south to north, and sub-humid and humid areas from north-west to south-east. The large precipitation and temperature gradients support diverse forest ecosystems ranging from evergreen broad-leaved and coniferous forests to deciduous coniferous and broad-leaved forests. Here, we selected 10 permanent plots with long-term observational data from CERN to cover the typical forest types with various ages in this region (Figure 1; Table S1). All 10 sites are well protected and subject to minimal disturbance.

2.2 | Data

The collected data are divided into four meteorological driving data, five stock-related constraint datasets of soil, foliage, fine root, wood, and leaf area index (LAI), and three flux-related constraint datasets of litterfall, net ecosystem exchange (NEE), and soil respiration (Rs). The time-series observations at most of the sites cover the period from 2005 to 2015, but those of SNF, which was incorporated into CERN later, are from 2010 to 2015 (Table S2).

2.2.1 | Biometric data

At each site, the biomass of leaves, branches, stems, and roots were estimated from the measured diameters at breast height and tree heights using the allometric method. The biomass inventory was performed at least once every 5 years. To split fine and coarse root biomass, the ratio of the fine root biomass to the entire root biomass in typical Chinese forests was obtained from Zhang and Wu (2001), and the coarse root biomass was then combined with the branch and stem biomasses to constitute the woody biomass. Estimates of leaf, fine root, and woody biomass were used to constrain the corresponding C pools in the inverse analysis.

The aboveground litterfall biomass was measured by 10 replicates of 100 cm × 100 cm baskets monthly during the growing season or once during the non-growing season. All collected litter was dried at 70°C for 24 hr and weighed. We used annual litterfall biomass data for the inverse analysis to avoid the effect of wind on the measurement of litterfall biomass within an individual month.

The LAI at each site was measured optically with a LAI-2000 plant canopy analyzer (LI-COR, Lincoln, NE, USA) at least quarterly every year and corrected by the foliage clumping index, which was set for plant functional type (PFT)-specific empirical values as reported in Zhu et al. (2012). The seasonal variation in the LAI combined with the leaf C mass per leaf area (LCMA) parameter constrained the dynamic trajectory of the leaf C pool in the MDF analysis.

2.2.2 | Soil data

Soil C content was calculated from soil organic matter (SOM) measured by the potassium dichromate oxidation titrimetric method and

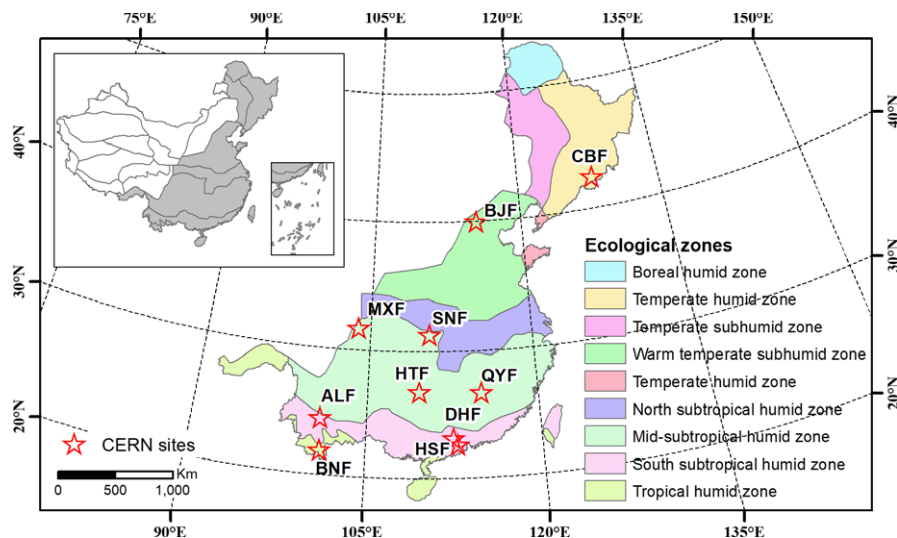


FIGURE 1 Map showing the distribution of 10 forest ecosystems in the Chinese Ecosystem Research Network (CERN). BNF: Xishuangbanna tropical seasonal rainforest; HSF: Heshan subtropical evergreen broad-leaved forest; DHF: Dinghu Mountain subtropical evergreen coniferous and broad-leaved mixed forest; ALF: Ailao subtropical evergreen broad-leaved forest; QYF: Qianyanzhou subtropical evergreen artificial coniferous mixed forest; HTF: Huitong subtropical evergreen broad-leaved forest; SNF: Shennongjia subtropical evergreen deciduous broad-leaved mixed forest; MXF: Maoxian warm temperate deciduous coniferous mixed forest; BJF: Beijing warm temperate deciduous broad-leaved mixed forest; CBF: Changbai Mountain temperate deciduous coniferous and broad-leaved mixed forest [Colour figure can be viewed at wileyonlinelibrary.com]

soil bulk density measured by the cutting ring method in each field campaign at 10 forest sites. At least three samples were collected from each of five soil layers (0–10, 10–20, 20–40, 40–60, and 60–100 cm) once every 5 years. We calculated the soil organic C (SOC) as follows (Post, Pastor, Zinke, & Stangenberger, 1985; Equation 1).

$$\text{SOC} = \sum_{i=1}^n 0.58 \times H_i \times B_i \times O_i \times 100 \quad (1)$$

where SOC is soil organic C density (g C m^{-2}) of all n layers, H_i is soil thickness (cm), B_i is soil bulk density (g cm^{-3}), and O_i is SOM content of the i th layer (%).

2.2.3 | Flux data

Net ecosystem exchange data were obtained from ChinaFLUX, covering CBF, QYF, ALF, and BNF. The data were aggregated to the daily time step from half-hourly CO_2 flux data measured by the eddy covariance technique and processed by quality control and gap filling (Li et al., 2008). To reduce the impact of gap-filled data on parameter estimations, we only aggregated NEE data for the days with at least 50% observed half-hourly fluxes, which were relatively evenly distributed in the daytime and nighttime.

Soil respiration data were measured using static chamber-gas chromatography techniques at CBF, QYF, DHF, HSF, and BNF (Zheng et al., 2010). A total of four to six replicates were measured two to three times per month with sampling times between 9:00 a.m. and 11:00 a.m. In this study, the monthly averaged heterotrophic respiration (R_h) was obtained according to the ratio of root respiration to R_s in the typical Chinese forest ecosystem to constrain the seasonal variation of C efflux from litter and soil in the inverse analysis (Chen, Yang, Ping-Ping, & Zhang, 2008).

2.2.4 | Meteorological data

In situ observations of daily air temperature (T), photosynthetically active radiation (PAR), relative humidity (RH), and saturated vapor pressure difference (VPD) at the 10 sites from 2005 to 2015 were obtained from the CERN scientific and technological resources service system (<http://www.cern.org.cn/>) and processed by standardized quality control and gap filling (Li et al., 2008; Liu, Tang, et al., 2017).

2.3 | Model

Data Assimilation Linked Ecosystem Carbon (DALEC) has been applied extensively in the MDF framework (Bloom et al., 2016; Richardson et al., 2010). It is a box model of C pools connected via fluxes running at a daily time step, and its main structure (i.e., C cycle, C allocation, and turnover process) is generally consistent with the state-of-the-art process-based models (Figure 2). Here, we used two versions of DALEC, an evergreen forest-specific version (DALEC-E; Williams, Schwarz, Law, Irvine, & Kurpius, 2005) with five pools (i.e., foliage, fine root, woody [including branch, stem, and coarse root], litter, and SOM) and a deciduous forest-specific version (DALEC-D; Fox et al., 2009) with an additional labile pool of stored C that supports leaf flushing.

The detailed C cycle of forest ecosystems can be characterized by several properties (Xia et al., 2013): (a) the C cycle is usually initiated with the canopy C influx GPP. Specifically, GPP is estimated herein using a canopy photosynthesis model (Ji, 1995; Appendix S1), which is a function of LAI, PAR, T, and RH. Note that the daily LAI is estimated as the ratio of the simulated foliar C pool and optimized

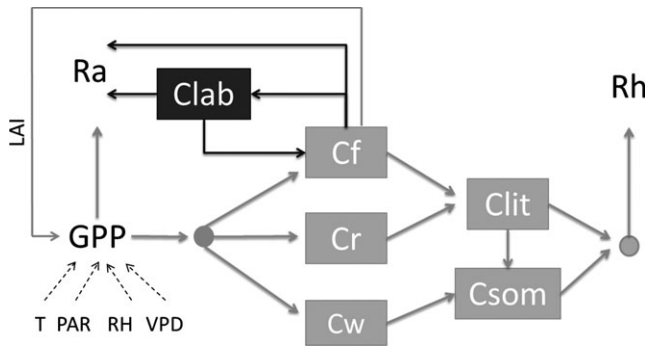


FIGURE 2 Structures of the Data Assimilation Linked Ecosystem Carbon (DALEC)-evergreen model (gray) and the DALEC-deciduous model (gray and black). Dotted arrows show the inputs into the photosynthesis model

LCMA parameter. (b) GPP is consumed in a certain fraction (f_{auto}) as autotrophic respiration (R_a) and partitioned into various plant pools (i.e., foliar, labile, wood, and fine roots); then, the degraded C from biomass pools goes to two dead organic matter pools with temperature-dependent losses (R_h). (c) C transfers are dominated by the donor pools (e.g., the litter decomposing into soil). (d) C exiting from C reservoirs is based on the first order differential equation. These properties of the forest C cycle in DALEC can be mathematically described by a matrix model as Equation 2 and determined as a function of key C cycle parameters (Table S3). All these parameters will be optimized based on the stock- and flux-related observations.

$$\frac{dC}{dt} = B I(t) - A \xi k C(t) \quad (2)$$

where $C(t)$ is a vector of C pool sizes at time t ; $B = (f_{\text{fol}}, f_{\text{root}}, f_{\text{woo}}, 0, 0)^T$ represents the partitioning fractions from photosynthetically fixed C input to the foliage (f_{fol}), root (f_{root}), woody (f_{woo}), litter, and soil pools; $I(t)$ is the input flux of fixed C via plant photosynthesis; $k = \text{diag}(\theta_{\text{fol}}, \theta_{\text{root}}, \theta_{\text{woo}}, \theta_{\text{min}} + \theta_{\text{lit}}, \theta_{\text{som}})$, a diagonal matrix of exit rates to quantify the fraction of C left from the foliage (θ_{fol}), root (θ_{root}), woody (θ_{woo}), soil (θ_{som}), litter (θ_{lit}) pool, and the litter mineralization rate into soil (θ_{min}); and $\xi = \text{diag}(1, 1, f(T), f(T))$, a diagonal matrix of temperature scalar $f(T)$ to quantify response of C decay rate to changes in temperature. The response to soil moisture was not considered in DALEC given the overall good moisture condition in these forest ecosystems ($\text{MAP} = 1,160.18 \pm 413.79$ mm). A is a square matrix of transfer coefficients to quantify C movement among pools as follows:

$$A = \begin{pmatrix} 1 & 0 & 0 & 0 & 0 \\ 0 & 1 & 0 & 0 & 0 \\ 0 & 0 & 1 & 0 & 0 \\ -1 & -1 & 0 & 1 & 0 \\ 0 & 0 & -1 & -\frac{\theta_{\text{min}}}{\theta_{\text{min}} + \theta_{\text{lit}}} & 1 \end{pmatrix} \quad (3)$$

2.4 | Estimation of ecosystem MTT and NEP based on the MDF framework

The analytical framework developed here systematically considered the C pool initial state, cost function, observational and forcing data

involved in the inverse analysis, and formula for estimating MTT to diagnose the SSA-induced bias in contrast to the NSSA, which affected parameter retrieval and the estimation of MTT and NEP (Figure 3). Note that models were the same in the NSSA and SSA setups. The temporal domains for model simulation were from 2005 to 2015.

2.4.1 | Parameter estimation under the SSA and NSSA

Under the NSSA, C pools are time-variant, that is, C influx is not equal to the C efflux, thus not restricted to $\text{NEP} \sim 0$; the dynamic long-term observations of C stocks and fluxes were used to constrain the DALEC model. As an important factor that may affect the estimated MTT and NEP, the initial state of the C pools was determined by the initial observation of C stocks or optimized (i.e., the labile pool, which cannot be directly observed) to avoid the uncertainty arising from the spin-up process. Then, the turnover and allocation parameters were inverted under the disequilibrium state (Equation 3) with dynamic environmental forcing.

$$\begin{cases} \frac{dC}{dt} \neq 0 \\ C_i(t+1) = C_i(t) + I_i(t) - k_i C_i(t), \quad i = 1, 2, \dots, n \\ C_i(t=0) = C_{i0} \end{cases} \quad (4)$$

where C_i , I_i , k_i represent the size, input, and turnover rate of the i th C reservoir, respectively; C_{i0} represent the initial state of the i th C reservoir; and t represent the daily step. According to the Bayesian theory, the posterior distributions of parameters are calculated by maximizing the likelihood function (Equation 4).

$$L_{\text{NSSA}} = \prod_{j=1}^m \prod_{i=1}^{n_j} \frac{1}{\sqrt{2\pi}\sigma_j} e^{-\frac{(x_{ji} - \mu_{ji}(P_{\text{NSSA}}))^2}{2\sigma_j^2}}, \quad m = 1, 2, \dots, 8 \quad (4)$$

where L_{NSSA} is the integrated likelihood function under the NSSA; m is the number of multiple data types; n is the number of data points in the j th data type; x_{ji} is the measured value composed of eight dynamic C stock and flux observations; $\mu_{ji}(P_{\text{NSSA}})$ represents the modeled fluxes and stocks based on parameters under the NSSA (P_{NSSA}); and σ_j is the standard deviation of each data point in the j th data type.

Under the SSA, C pools are stabilized such that an additional constraint of long-term $\text{NEP} \sim 0$ was used to constrain the initial state of C pools at steady state, in addition to the observed C stock and flux constraints. As the meteorological forcing spans 2005–2015, we averaged total ecosystem C pools (C_{TOT}) over each 10-year segment to obtain $\overline{C_{\text{TOT}}}$, and determined steady state criterion by which changes in $\Delta \overline{C_{\text{TOT}}}$ (Equation 5) between two neighboring segments are within a threshold of $0.5 \text{ g C m}^{-2} \text{ year}^{-1}$ (as one criterion in Thornton & Rosenbloom, 2005; Xia et al., 2012).

$$\overline{\Delta C_{\text{TOT}}} = |\overline{C_{\text{TOT}}(t+1)} - \overline{C_{\text{TOT}}(t)}| \leq 0.5 \quad (5)$$

where t represents the period for parameter optimization during 2005–2015.

The C turnover and allocation parameters were retrieved under the repeated 10 year (2005–2015) cycle of meteorological forcing until the initial state of C pools were stationary at the annual time

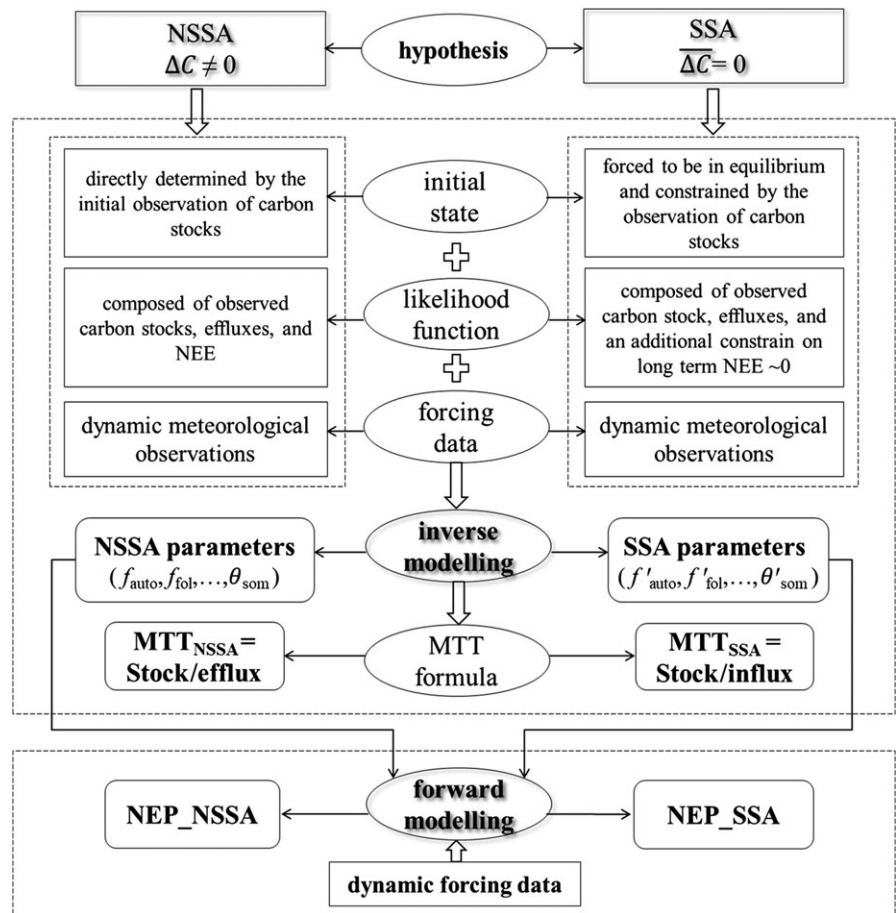


FIGURE 3 Flow chart of the model-data fusion framework under the steady state assumption (SSA) and non-steady state assumption (NSSA)

scales (i.e., long-term NEP ~ 0 , Equation 5), and the likelihood function was maximized compared to the observations (Equation 6).

$$L_{SSA} = \prod_{j=1}^m \prod_{i=1}^{n_j} \frac{1}{\sqrt{2\pi\sigma_j}} e^{-\frac{(x_{ij} - \mu_{ij}(P_{SSA}))^2}{2\sigma_j^2}}, \quad m = 1, 2, \dots, 8 \quad (6)$$

where $\mu_{ij}(P_{SSA})$ represents the modeled values based on parameters under the SSA (P_{SSA}), and L_{SSA} is the integrated likelihood under the SSA and consists of five stock-related observations, two efflux observations (litterfall and Rs), and the tolerance of long-term NEE described in Equation 5.

Specifically, we applied the Metropolis simulated annealing algorithm, a variation of the Markov Chain Monte Carlo technique, for parameter estimation (Zobitz, Desai, Moore, & Chadwick, 2011). Besides, ecological and dynamic constraints were imposed on the DALEC parameters and pool dynamics (Appendix S2) which can significantly reduce uncertainty in model parameters and simulations (Bloom & Williams, 2015).

2.4.2 | Estimation of ecosystem MTT under the SSA and NSSA

Here, we use the MTT_(MDF scheme, i.e., SSA/NSSA) (flux term used, i.e., Input (I) /Output (O)) to consistently define the C turnover times in

different analyses. Under the SSA, long-term NEP = 0; that is, the C influx equalizes the efflux, such that the ecosystem MTT can be defined as the ratio of retrieved total ecosystem C stocks to the ecosystem influx (Sanderman, Amundson, & Baldocchi, 2003, Equation 7):

$$MTT_{SSA,I} = \frac{\overline{C_{pool_SSA}}}{I_{SSA} - \Delta C_{pool}} = \frac{\overline{C_{pool_SSA}}}{I_{SSA}} \quad (7)$$

where MTT_{SSA,I} is the ecosystem MTT under the SSA as estimated from C influx, $\overline{C_{pool_SSA}}$ is the mean annual ecosystem C pool, I_{SSA} is the mean annual ecosystem C input (GPP), and ΔC_{pool} is the change in the ecosystem C pool.

We have further derived an analytical expression for MTT_{SSA,I} (Equation 8):

$$\begin{aligned} MTT_{SSA,I} &= \frac{\sum_i \overline{C_{pool_i_SSA}}}{I_{SSA}} = \frac{\overline{I_{i_SSA}}}{I_{SSA}} \times \frac{\sum_i \overline{C_{pool_i_SSA}}}{\overline{I_{i_SSA}}} \\ &= \left(\frac{f_{fol}}{\theta_{fol}} + \frac{f_{roo}}{\theta_{roo}} + \frac{f_{woo}}{\theta_{woo}} + \frac{f_{fol} + f_{roo}}{(\theta_{min} + \theta_{lit}) \times \xi} + \frac{f_{woo} + (f_{fol} + f_{roo}) \times \frac{\theta_{min}}{\theta_{min} + \theta_{lit}}}{\theta_{som} \times \xi} \right) \\ &\quad \times (1 - f_{auto}) = (1 \quad 1 \quad \dots \quad 1)(A\xi k)^{-1} B(1 - f_{auto}) \end{aligned} \quad (8)$$

where $\overline{C_{pool_i_SSA}}$ and $\overline{I_{i_SSA}}$ represent the mean annual size and influx of the i th C pool, respectively, which are simulated based on the site-specific SSA-optimized parameters at each site.

This form is compatible with the inverse matrix composed of the optimized allocation, turnover, and transit parameters (Luo et al., 2017; Xia et al., 2013), which consider the ecosystem MTT to be aggregated from the sum of turnover times for pools in series and the influx-weighted turnover time of pools in parallel (Barrett, 2002). The inherent consistency is theoretically supported by Sierra, Müller, Metzler, Manzoni, and Trumbore (2017), because both forms are based on the hypothesis that the size of the C pool is equivalent to the product of C input flux and C turnover time in the equilibrium state (Bolin & Rodhe, 1973).

Under the NSSA, each C pool is an instantaneous state variable; thus, the efflux-weighted turnover time of pools is also time-variable and cannot be parameterized. Therefore, constructing an inverse matrix explicitly composed of the turnover and allocation parameters to represent the MTT is difficult. In this case, the ratio of the total ecosystem C stock to the efflux simulated based on these optimized parameters under NSSA is used to estimate ecosystem MTT (Schwartz, 1979; Bloom et al., 2016; Equation 9).

$$\begin{aligned} \text{MTT}_{\text{NSSA}_O} &= \frac{\overline{C_{\text{pool}_{\text{NSSA}}}}}{\overline{I_{\text{NSSA}} - \Delta C_{\text{pool}}}} = \frac{\overline{C_{\text{pool}_{\text{NSSA}}}}}{\overline{O_{\text{NSSA}}}} \\ &= \frac{\sum_i^n \overline{C_{\text{pool}_i}_{\text{NSSA}}}}{\overline{O_{\text{NSSA}}}} = \frac{\overline{O_{i_{\text{NSSA}}}}}{\overline{O_{\text{NSSA}}}} \times \frac{\sum_i^n \overline{C_{\text{pool}_i}_{\text{NSSA}}}}{\overline{O_{i_{\text{NSSA}}}}} \quad (9) \\ &= (1 \quad 1 \quad \dots \quad 1)(\xi k)^{-1} w \end{aligned}$$

where $w = \left(\frac{\overline{O_{\text{fol}_{\text{NSSA}}}}}{\overline{O_{\text{NSSA}}}}, \frac{\overline{O_{\text{woo}_{\text{NSSA}}}}}{\overline{O_{\text{NSSA}}}}, \frac{\overline{O_{\text{roo}_{\text{NSSA}}}}}{\overline{O_{\text{NSSA}}}}, \frac{\overline{O_{\text{lit}_{\text{NSSA}}}}}{\overline{O_{\text{NSSA}}}}, \frac{\overline{O_{\text{som}_{\text{NSSA}}}}}{\overline{O_{\text{NSSA}}}} \right)$; $\text{MTT}_{\text{NSSA}_O}$ is the ecosystem MTT under the NSSA based on C output; $\overline{C_{\text{pool}_{\text{NSSA}}}}$ is the mean annual ecosystem C pool; $\overline{I_{\text{NSSA}}}$ is the mean annual ecosystem C input (GPP); $\overline{O_{\text{NSSA}}}$ is the mean annual ecosystem C output (RE); $\overline{C_{\text{pool}_i}_{\text{NSSA}}}$ and $\overline{O_{i_{\text{NSSA}}}}$ represent the mean annual size and output of the i th C pool, respectively; w represents the output-dependent weight of C pools; and $\overline{O_{\text{fol}_{\text{NSSA}}}}$, $\overline{O_{\text{woo}_{\text{NSSA}}}}$, $\overline{O_{\text{roo}_{\text{NSSA}}}}$, $\overline{O_{\text{lit}_{\text{NSSA}}}}$, and $\overline{O_{\text{som}_{\text{NSSA}}}}$ represent the mean annual output of the foliage, wood, root, litter, and soil pools, respectively. All C stocks and fluxes were simulated based on the site-specific NSSA-optimized parameters at each site. Because the C reservoirs, fluxes, and turnover times are instantaneous values, we used the average of the fluxes and reservoirs for multiple years to reflect the average turnover time during a specific period (i.e., 2005–2015). Note that with few natural and anthropogenic disturbances at these well-protected CERN sites (Zhang et al., 2010; Zhou et al., 2006), the total ecosystem output was approximately equivalent to the RE.

2.4.3 | Estimation of ecosystem NEP based on the SSA- and NSSA-inverted parameters

The optimized parameter values under the NSSA and SSA along with the initial observations of corresponding C pool sizes were used in forward modeling driven by the dynamic environmental variables from 2005 to 2015 (Zhou & Luo, 2008). NEP was further derived from the difference between the ecosystem C influx and RE to examine the effects of retrieved parameters on C sequestration under different hypotheses.

2.5 | Estimation of ecosystem MTT based on observation

To test the robustness of $\text{MTT}_{\text{SSA}_I}$ based on SSA-inversion at the 10 sites, the MTT under the SSA based on observed influx ($\text{MTT}_{\text{OBS}_I}$) was calculated from the ratio of mean annual total ecosystem stock measurements in CERN and the mean annual GPP observed from moderate resolution imaging spectroradiometer (MODIS) (Carvalho et al., 2014). MODIS products of GPP (MOD17A2H, 500m) at each site were downloaded from the University of Oklahoma Data Center (<http://www.eomf.ou.edu/visualization/manual/>) and then accumulated to the annual time step from the 8-day observational data. Because the annual MODIS GPP values are consistent with the tower-based GPP at the flux sites (Figure S1, $R^2 = 0.90$, $p < 0.01$, mean absolute error [MAE] = 37.39 g C m⁻² year⁻¹), it is reasonable to use this high-resolution product as a reliable observation at the site scale.

3 | RESULTS

3.1 | Key parameters retrieved under the SSA and NSSA

Under the NSSA, the ratio of Ra to GPP (f_{auto}) varied from 0.3 to 0.7, with a mean value of 0.53, showing a trend of first decreasing and then increasing with decreasing latitude (Figure 4a and Figure S2). The proportion of NPP allocated to wood (f_{woo}) ranged from 0.5 to 0.9, with a mean value of 0.67, showing an increasing trend with decreasing latitude (Figure 4d and Figure S2). The MTTs (i.e., the inverse of the turnover rate) of wood, soil, foliage, fine root, and litter at the 10 sites were 48.54, 86.55, 3.12, 2.40, and 1.13 years, respectively. Specifically, the turnover rate of wood and soil (θ_{woo} and θ_{som}), the two largest C pools in living vegetation and dead organic matter, respectively, showed obvious increasing trends with decreasing latitude (Figure 4g,i and Figure S2). The temperature sensitivity of soil decomposition (Rh_{temp}) exhibited a spatial pattern of tropical forest > temperate forest > subtropical forest (Figure 4k and Figure S2). However, compared to the key C cycle parameters under the NSSA, the allocation to faster-turnover C pools under the SSA was mostly overestimated (f_{auto} , f_{fol}), but to slow-turnover pools (f_{woo}) was underestimated; turnover rate of major pools (θ_{woo} and θ_{som}) were overestimated; furthermore, the sensitivity to climate (Rh_{temp}) was underestimated; and these parameters lacked obvious spatial patterns (Figure 4a,c,d,g,i,k).

We compared the modeled and observed datasets to validate the inverted parameters based on multi-source data. Under the NSSA, the simulated and observed vegetation and soil C stocks and C fluxes agreed well, with the scatter points falling along the 1:1 line (Figure 5). Specifically, the determination coefficients (R^2) for C stocks varied between 0.94 and 0.99, and the root-mean-square errors (RMSEs) were small relative to their magnitudes (Figure 5a–e). In contrast, R^2 for C fluxes (NEE and R_s) were slightly lower (0.45–0.50), but the RMSEs were only 1.37 and 0.67 g C m⁻² day⁻¹,

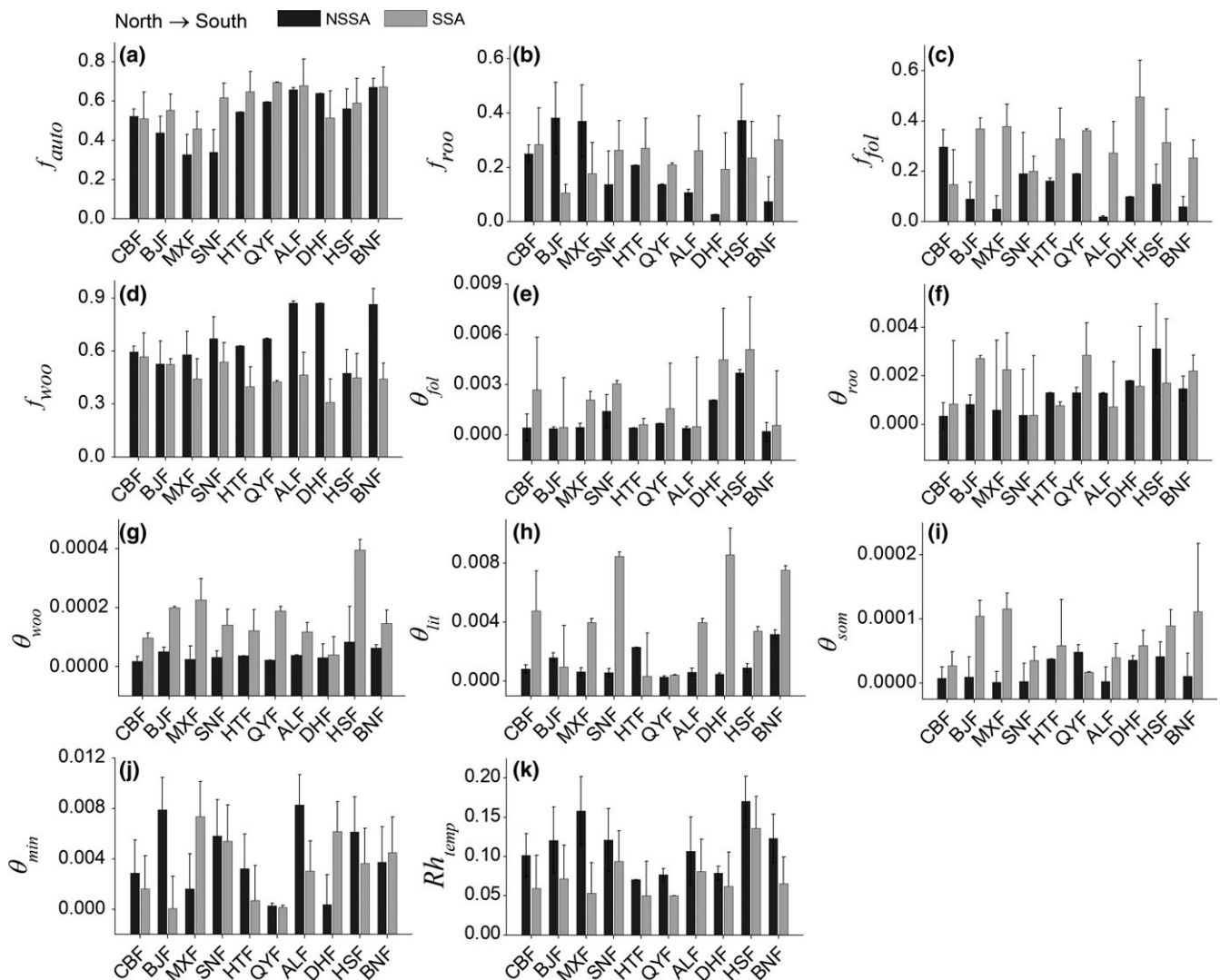


FIGURE 4 Optimized key parameters involved in the allocation and turnover processes under the non-steady state assumption (NSSA) and steady state assumption (SSA) at 10 sites along a decreasing latitudinal gradient. The black and gray boxes denote NSSA and SSA, respectively

respectively (Figure 5g,h). Under the SSA, the model performance regarding the C stocks was comparable with that under the NSSA (Figure 5a–e), but due to the overestimation of C turnover rates (Figure 4e–j), simulated C effluxes, such as litterfall and R_s , were markedly overestimated, which in turn overestimated NEE (Figure 5f–h).

3.2 | Magnitude of MTT and its relationship with forest age under the SSA and NSSA

At the 10 sites, the MDF-based ecosystem MTT under NSSA (MTT_NSSA_O) and SSA (MTT_SSA_I) and the observation-based ecosystem MTT under SSA (MTT_OBS_I) ranged from 9.64 to 38.23, 7.29 to 33.59, and 8.73 to 36.31 years, with averages of 24.44, 17.27, and 17.20 years, respectively. As MTT_SSA_I and MTT_OBS_I were nearly identical (Figure 6b, MAE = 0.25, $R^2 = 0.86$, $p < 0.001$), MTT_SSA_I was selected to represent the estimated MTT under SSA in the ensuing analyses.

The ecosystem MTT_SSA_I was significantly lower (with an average of 29%) than the MTT_NSSA_O (Figure 6a, $p < 0.05$). Because wood and soil are the two largest C pools in forest ecosystems, the differences in their turnover rates estimated under the SSA and NSSA and the relative contributions to the difference between the whole-ecosystem MTT_SSA_I and MTT_NSSA_O (Δ MTT) deserved further analysis. Both the θ_{woo} and θ_{som} were significantly overestimated under the SSA (Figure 4g,i) with the magnitude of the overestimation for θ_{woo} being greater than that for θ_{som} ($1.24E-04$ vs. $5.02E-05$), which largely accounted for the ecosystem Δ MTT. Meanwhile, less C was allocated to slow-turnover structural C pools under the SSA (Figure 4d, $f_{woo_SSA} = 0.46$ vs. $f_{woo_NSSA} = 0.68$), thus leading to underestimations of the vegetation MTT and ecosystem MTT.

The ecosystem Δ MTT varied among different ecosystems (Figure 6a), and these differences should be closely associated with how far the ecosystems deviate from the equilibrium state, as most likely reflected by the age-related growth. Thus, forest age was used as a

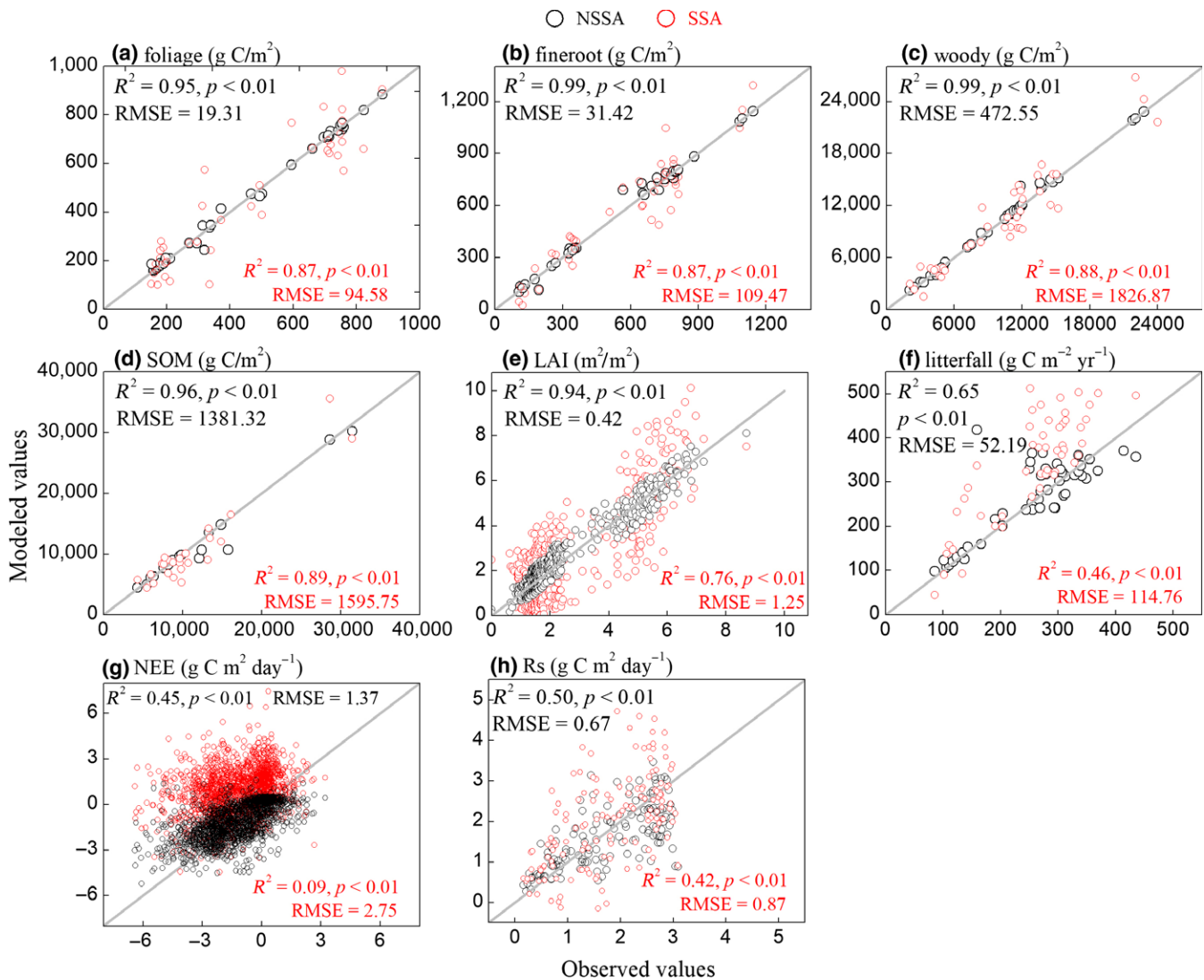


FIGURE 5 Comparisons between the observed and modeled values at all sites under the non-steady state (NSSA: black dots) and steady state (SSA: red dots) assumptions [Colour figure can be viewed at wileyonlinelibrary.com]

proxy of the gap between the actual and equilibrium state. We found that the forest age accounted for more than 50% of the variation in ecosystem Δ MTT with a significantly negative correlation (Figure 7a, $p < 0.005$). Further analysis revealed that rather than the overestimation of θ_{som} , the overestimation of θ_{woody} under the SSA ($\Delta\theta_{\text{woody}}$), which exhibited a significant power function relationship with forest age, dominated the age-dependent Δ MTT in the entire ecosystem (Figure 7b and Figure S3).

3.3 | Latitudinal pattern of MTT and its covariance with climate under the SSA and NSSA

The ecosystem MTT_{NSSA_O} and MTT_{SSA_I} exhibited similar latitudinal patterns, both of which decreased with decreasing latitude (Figure 8a), showing a pattern of temperate MTT > subtropical MTT > tropical MTT (Figure 6a). ALF appears to be an outlier, mainly due to its high elevation (2,488 m) and special vertical

zonal. We further analyzed the relationship between MTT and climate, which is recognized as an important factor regulating the latitudinal MTT gradient (Carvalho et al., 2014). Both the ecosystem MTT_{SSA_I} and MTT_{NSSA_O} were negatively correlated with temperature and precipitation (Figure 8b,c), but the sensitivity of the MTT_{SSA_I} to these two climatic variables was significantly lower than that of the MTT_{NSSA_O}, which decreased from 1.02 to 0.80 year/°C (by 22%) for temperature and from 1.34 to 0.78 year/100 mm (by 42%) for precipitation.

3.4 | Ecosystem C sequestration based on the SSA- and NSSA-inverted parameters

Under the dynamic environmental conditions, all 10 forests were net C sinks based on both the SSA- and NSSA-inverted parameters (Figure 9). However, with respect to actual eddy covariance observations, the NEP was obviously underestimated with the SSA-inverted

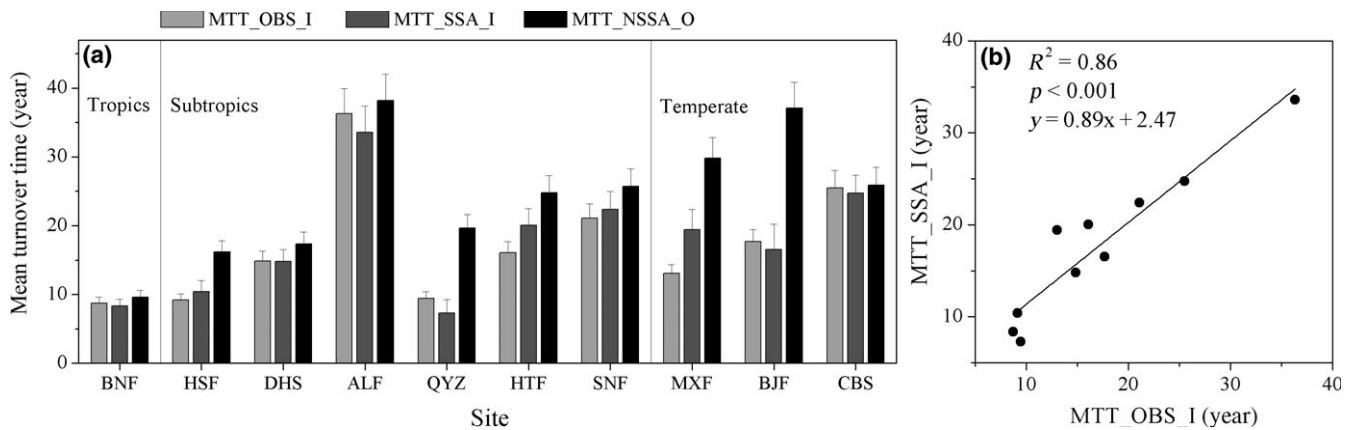


FIGURE 6 Magnitude of ecosystem C turnover times under the equilibrium and disequilibrium hypotheses. The black, light-gray, and dark gray boxes denote the inversion-based MTT under non-steady state (MTT_NSSA_O), inversion-based MTT under steady state (MTT_SSA_I), and observation-based MTT under steady state (MTT_OBS_I), respectively

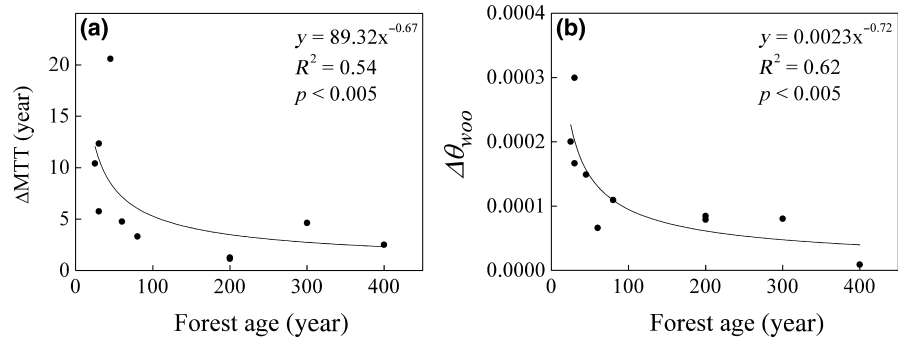


FIGURE 7 Relationships between forest age and differences of the entire ecosystem MTT (Δ MTT) as well as wood turnover rates ($\Delta\theta_{wood}$) estimated under the steady state assumption (SSA) and non-steady state assumption (NSSA) hypotheses

parameters, whereas the NEP based on NSSA parameters was highly consistent (Figure 5g); for example, the mean annual NSSA-estimated and observed NEP were 347.4 and $306.6 \text{ g C m}^{-2} \text{ year}^{-1}$ at CBF, respectively, and 465.9 and $469.3 \text{ g C m}^{-2} \text{ year}^{-1}$ at QYF. Overall, the mean annual NEP for 10 typical forest ecosystems in eastern China monsoon region reached $325.2 \text{ g C m}^{-2} \text{ year}^{-1}$ based on NSSA-inverted parameters, which was 4.83 times that estimated with SSA-inverted parameters ($67.3 \text{ g C m}^{-2} \text{ year}^{-1}$). Furthermore, the SSA-induced bias in NEP was significantly greater ($p < 0.05$) in young and middle-aged forests (7.3-fold) than that in mature forests (3.8-fold). The underestimation of NEP in SSA analysis was largely due to the overestimation of RE, which is closely associated with the overestimation of C turnover rates and allocations to fast-turnover pools (Figure 4); whereas GPP was comparable to that under the NSSA (Figure S4).

4 | DISCUSSION

4.1 | Robustness of MTT estimations under SSA and NSSA

The robustness of MTT_SSA_I estimations in the 10 ecosystems has been assessed with respect to MTT_OBS_I, which is generally recognized as a benchmark in current research (e.g., Thurner et al., 2017).

Although eddy covariance measurements for MTT_OBS_I estimation are lacking for some of the sites, the MOD17A2H product performed as a suitable alternative for GPP observations because its spatial resolution is finer than the footprint of the flux towers (Mi, Yu, Wang, Wen, & Sun, 2006; Zhao et al., 2005). Furthermore, we found the magnitude and spatial pattern of ecosystem MTT_SSA_I in eastern China monsoon forests were consistent with various MTT_SSA estimations by observation or inversion approach in regional or global forest ecosystems (Table S4). A negative correlation of MTT_SSA_I with both temperature and precipitation was observed in this study, which was supported by research on MTT_SSA_I based on forest inventory and remote sensing observations (Carvalho et al., 2014; Gill & Jackson, 2000; Sanderman et al., 2003). The high consistency and robustness of MTT_SSA calculated by various methods indicated that the deviation in MTT_SSA identified in this study has broad implications for various SSA applications in C cycle research.

Due to the complexity of ecosystem C emission processes and the scarcity of ecosystem efflux data, it remains challenging to validate the inverted MTT_NSSA_O of whole-ecosystem with respect to observation-based estimates at disequilibrium state. However, the magnitude of the key process parameters regulating the ecosystem MTT under the NSSA as inferred in this study was broadly consistent with a number of empirical studies on C allocations, vegetation

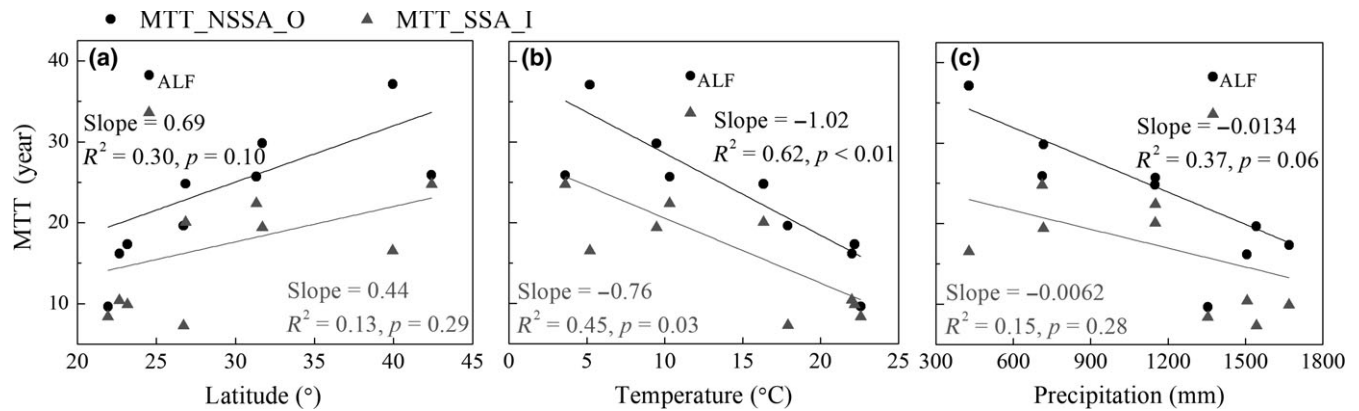


FIGURE 8 Associations of mean carbon turnover times with temperature and precipitation under the steady state assumption (SSA, gray triangles) and non-steady state assumption (NSSA, black dots)

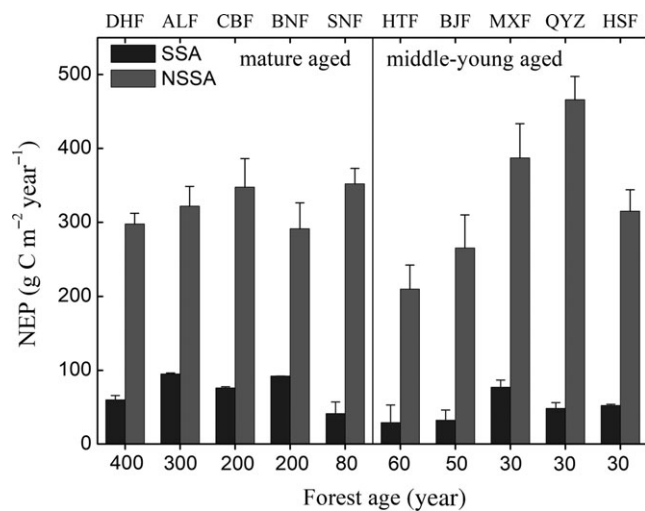


FIGURE 9 Comparison of net ecosystem productivity (NEP) estimated with the parameters inverted under the steady state assumption (SSA) and non-steady state assumption (NSSA) in 10 forest ecosystems of different ages

turnover rates and mortality, and soil decomposition rates (Table S5). The turnover times of fine roots measured from $\delta^{13}\text{C}$ signals tend to be systematically overestimated due to sampling biases, with the finest and most ephemeral roots being missed (Strand, Pritchard, McCormack, Davis, & Oren, 2008). Regarding the pattern of these key processes, f_{auto} first decreased and then increased as temperature increased at the turning point of approximately 11°C , which was highly congruent with the synthetic analysis based on the global forest database and could be ascribed to the asymmetric response of RE and GPP to rising temperature (Piao et al., 2010). The decrease in f_{woo} with increasing latitude and decreasing temperature was supported by the inventory-based synthesis in Chinese forests (Li, Zhou, & He, 2009), and this pattern may be explained by the adaptive strategies of forest trees to temperature (Reich et al., 2014) as well as the age-structure-related strategy (Zhou, Shi, et al., 2013), which tends to allocate less C to the structural pool in old forests mainly distributed in cold, high-latitude regions in China (Zhang et al.,

2014). θ_{woo} and θ_{som} both increased with rising temperature, which agrees well with the variation in the plant mortality rate based on forest inventory (Mantgem et al., 2009; Zhou, Peng, et al., 2013) and the variation in soil C decomposition based on Rs observations from the chamber or isotope method (Chen, Huang, Zou, & Shi, 2013; Frank, Pontes, & McFarlane, 2012; Karhu et al., 2010). In addition, R_{temp} was higher in tropical and temperate forests than subtropical forests, which is consistent with the regional variation in temperature sensitivity in Chinese forests based on field sampling and incubation experiments (Liu, He, et al., 2017; Zhou et al., 2009).

Overall, the robustness of estimations under the NSSA compared to the empirical research indicates that the C cycle dynamics estimated by NSSA method match the realistic observations well. Thus, the SSA-induced bias in MTT estimation and the underlying mechanism can be reliably quantified in contrast to our estimations under NSSA.

4.2 | Identification of the uncertainty in MTT under SSA

Under the background of global environmental changes, extensively distributed disturbances drive the ecosystems far from a steady state at local scales (Luo & Weng, 2011), which makes the spatially specific research a great challenge. Although the spatial aggregation of regional/global may approximately estimate the MTT under the SSA (Odum, 1966), identifying the explanatory mechanism is difficult because the aggregation also merges some spatially heterogeneous influencing factors, such as temperature and terrain, that nonlinearly impact the MTT. In addition, previous studies have challenged the inherent concept behind SSA for the ecosystem C cycle (Cannell & Thornley, 2003; Lugo & Brown, 1986), for example, whether SSA-applicable old-growth forests are quasi-neutral or large C sinks (Luysaert et al., 2008; Zhou et al., 2006). Moreover, some uncertainties from the SSA have been revealed in C cycle studies; for example, model initialization until equilibrium systematically overestimated the C pools (Pietsch & Hasenauer, 2006), exhibiting a sixfold range among various global C models (Exbrayat et al., 2014). This further

led to compensatory biases in NEP simulation, whereas relaxing the SSA in initialization made a 92% decrease in NEP errors (Carvalhais et al., 2008, 2010). Besides, key turnover parameters determined under the SSA were overestimated, for example, the decay rate of recalcitrant pools (Wutzler & Reichstein, 2007); this further resulted in underestimation of NEP in transient simulation, which may be up to 30% even when C sinks only account for 10% of the C input in disequilibrium ecosystems (Zhou, Shi, et al., 2013). It is noteworthy that these biases in pool initialization and parameter inversion will propagate into the MTT estimation via the “pool/flux” method and need to be determined.

Our study provides a new MDF framework to trace the uncertainty in turnover time induced by traditional SSA through direct comparison with the realistic disequilibrium state rather than conducting sensitivity experiments as reported in Carvalhais et al. (2008) or Zhou, Shi, et al. (2013). Additionally, we collectively consider the factors resulting in the mismatch between MTT_{SSA_I} and MTT_{NSSA_O} , that is, the pool initialization, the turnover, and allocation parameter inversions as well as the formulas for estimating MTT used under two assumptions (Figure 3). Via this framework, a significant underestimation in MTT_{SSA_I} was observed in these sites, which may be partly explained by the overestimated turnover rates and underestimated allocation to structural pools under SSA (Figure 4). Moreover, in ecosystems with substantial sinks where GPP is much higher than RE, the input-based MTT_{SSA_I} should be smaller than the output-based MTT_{NSSA_O} , which might be more evident in younger forests due to the intrinsic relationship between age and forest growth (Goulden et al., 2011; Zaehle et al., 2006).

To further distinguish the SSA-induced biases arising from the parameterization or the MTT estimation, we contrasted MTT_{NSSA_O} versus MTT_{SSA_O} ($R^2 = 0.76$, RMSE = 9.01 year) and MTT_{NSSA_I} versus MTT_{SSA_I} ($R^2 = 0.74$, RMSE = 4.41 year) to obtain the biases that only stem from the improper use of SSA in parameterization. We found that these biases were much higher than those induced by only using SSA in MTT estimation, that is, MTT_{NSSA_I} versus MTT_{NSSA_O} , or MTT_{SSA_I} versus MTT_{SSA_O} (Table S6). This indicated that the effect of the improper SSA on parameterization was deeper than that on MTT estimation, which provides a significant caveat for SSA applied especially in model optimization (e.g., Barret, 2002; Zhou & Luo, 2008; Zhou et al., 2010; Zhou, Shi, et al., 2013). In the future, with the accumulation of spatiotemporal observations (Le Toan et al., 2011), we suggest evaluating the dynamic disequilibrium state of C cycle (e.g., Bloom et al., 2016), and further quantifying and reducing the SSA-induced uncertainty at large scales, especially with non-steady-state behavior, using this proposed framework.

4.3 | Implications of SSA-induced uncertainty in MTT for C cycle research

As a key factor determining the ecosystem C sequestration capacity, the uncertainty of MTT tends to dominate the uncertainty in terrestrial ecosystem C sequestration (Friend et al., 2014; He et al., 2016).

Thus, identifying the relative contribution of this highly uncertain ecosystem trait to C sequestration has become a hot topic in C cycle research (Carvalhais et al., 2014; Todd-Brown et al., 2013; Yan, Zhou, Jiang, & Luo, 2017). We employed a systematic framework and quantified that the deviation in MTT when improperly invoking SSA directly results in a pronounced underestimation of ecosystem NEP (4.83-fold) in this large C uptake region. The substantial underestimation of NEP found is supported by Yu et al. (2014), who revealed that state-of-the-art process-based models under the SSA tended to underestimate NEP by fivefold to sevenfold relative to eddy covariance observations in eastern Asia monsoon subtropical forests. Moreover, process-based models significantly underestimated NEP compared to other approaches, for example, biomass and soil inventory, and atmospheric inversion (Piao et al., 2009). This is mainly because the models consistently assume that the ecosystem has approached an equilibrium state, which obviously neglects age-structure-related effects and underestimates the turnover times at regional and global scales (Carvalhais et al., 2014; Thurner et al., 2017; Yan et al., 2014).

Here, we firstly reveal that the deviation in ecosystem MTT induced by SSA has a clearly decreasing relationship with increasing forest age. Furthermore, the biases in vegetation allocation and turnover, rather than those in soil turnover, dominate the magnitude of the deviation in MTT and its dependency on forest age. This finding is most likely due to the significantly stronger relationship between vegetation C turnover and stand age, whereas soil C turnover is mostly affected by climatic factors (Wang et al., 2018). In addition, the vegetation C partition scheme varies with stand age (Zhou, Shi, et al., 2013). The decisive role of whole-vegetation turnover time in determining the uncertainty in ecosystem C storage capacity has been supported by recent modeling and experimental research (Friend et al., 2014; Medlyn et al., 2015; Xue et al., 2017). Therefore, our results further highlight the need to focus on the deviation in vegetation C turnover time under the SSA to avoid considerable bias in ecosystem MTT and thus the C sequestration estimation.

The East Asian monsoon forest ecosystems represent one of the highest C uptake regions worldwide, including mid- and high-latitude European and North American forests. Particularly, the young age structure of forest stands in this region has been identified as a major driver of the large NEP (Yu et al., 2014). Therefore, our result offers a significant caveat for applying SSA in regions with a large portion of young ecosystems. We expect that improved representations of forest age-driven growth and mortality into calibrated process-based models will help reduce the aforementioned biases for the C balance of ecosystems regionally and globally. Additionally, our finding on the age-dependent deviation of MTT could also offer an opportunity to correct the MTT_{OBS_I} at regional or global scales (e.g., Thurner et al., 2016) with spatially explicit forest age information, thereby providing a better benchmark to inform or parameterize C cycle models.

In addition to the uncertainty in the magnitude of C storage capacity, previous studies have revealed that the major uncertainty in the response of ecosystem C storage to climate arises from the

uncertainty in the response of MTT to climate, which is 30% higher than that caused by NPP (Friend et al., 2014). However, to our knowledge, this is the first attempt to quantify the relationship between climate and ecosystem MTT in the disequilibrium state and to discuss the differences with that at the equilibrium state. Theoretically, an ecosystem at equilibrium is stable for a long time under the local climate (Luo & Wang, 2011); thus, a relatively strong correlation can be expected between the ecosystem MTT and climate. However, it is inappropriate to invoke the ideal SSA in ecosystems at dynamic disequilibrium, with the MTTs underestimated to a greater extent in young and middle-aged forests (by more than 50%) than mature forests (<20%). This age-induced inconsistency in MTT underestimations disturbs the actual spatial pattern of MTT and its covariance with climate, thereby leading to a decreased sensitivity of MTT to climate under the SSA. In contrast, the MTT_{NSSA} estimation based on long-term observational data in this study implicitly incorporated the age-structure-related effect on C cycle dynamics, thus providing a proper perspective on the actual correlation between MTT and climate. Currently, the contributions of climate-driven changes in C turnover times to C storage are usually underestimated in modeling studies (Hararuk, Smith, & Luo, 2015; Koven et al., 2015; Koven, Hugelius, Lawrence, & Wieder, 2017). Therefore, the substantial underestimation we revealed of sensitivities of MTT to temperature and precipitation induced by the SSA calls for more attention in future C-climate feedback research. Under global warming and changes in precipitation regimes (IPCC, 2013), the underestimated response of MTT to climate will apparently underestimate the spatial and temporal changes in MTT, thereby underestimating the change in predicted global NEP. Here, the exchange of space for time to interpret the sensitivity of MTT to climate could cause some degree of bias, as such inference cannot include certain processes like acclimation of microbial respiration to warming or shifts in plant species over time (e.g., Koven et al., 2017; Yan et al., 2017). Nonetheless, the present-day spatial correlation between climate and MTT approximated the temporal correlation between these variables (Figure S5) and well supported this inference.

4.4 | Advantages and challenges of C cycle MDF based on long-term data

Carbon turnover times and C cycle dynamics are always model-dependent because of the difficulty obtaining them from observations alone under the NSSA (Sierra et al., 2017). However, even the state-of-the-art models fail to accurately capture the observed C allocations and turnover processes, resulting in high uncertainties in C dynamic simulations (De Kauwe et al., 2014; Negrón-Juárez, Koven, Riley, Knox, & Chambers, 2015). Therefore, applying MDF technology to constrain these C states and processes becomes important for accurately estimating MTT and C sequestration in the disequilibrium state (Bloom et al., 2016).

The uncertainties in the current ecosystem MTT and C sequestration estimates mainly result from the lack of initial state of the C pools and inaccurate model parameters (Bellassen et al., 2011; Wang

et al., 2011), because C cycle modeling typically relies on pre-arranged parameters retrieved from literature, prescribed PFT or spin-up processes (Exbrayat et al., 2014; Zhou, Shi, et al., 2013). In this study, the long-term and multi-source observations combined with a series of experimental constraints directly provided the initial values of the corresponding C pools and better constrained the NSSA parameters and dynamic C pool trajectories (Bloom & Williams, 2015; Smallman et al., 2017), thus substantially reducing the uncertainties arising from the SSA and limited data. Furthermore, insights into the underlying mechanisms that regulate the ecosystem C cycle can be provided based on the key process parameters, which are difficult to obtain from observations without SSA. For example, we might explore how the C allocation and turnover in live and dead C respond to climate, thereby regulating the response of the whole-ecosystem MTT to climate (Figure S6).

The uncertainty from the model structure and observational data also induce errors in the estimations of ecosystem MTT and C sequestration (Ahlström, Schurgers, Arneeth, & Smith, 2012). However, as this study aimed to compare the differences in MTTs estimated under different hypotheses with the same model and data, these two factors would not undermine the main conclusions. When applied at the regional scale, some external disturbances such as fire and land-use change (Erb, 2016); vegetation mortality dynamics affected by drought, insect pests, and frost (Thurner et al., 2016); as well as the dynamic scheme of C allocation limited by resources availability (Xia, Chen, Liang, Liu, & Yuan, 2015) should be added to the model. Although the model without moisture effect did not significantly affect the results in these forests (Table S7), the explicit representation of moisture effect may improve the model simulation when applied at large scales. Besides, more underground process observations should be added in future research to better constrain the corresponding parameters, for example, θ_{\min} , reflecting the decomposition of litter into soil.

In this study, we provided insights into the large biases associated with the improper application of the SSA, causing considerable underestimation in the magnitudes of MTT and its sensitivities to climate, and spatiotemporal variations in ecosystem C sequestration. Our findings on the age-dependent uncertainty in MTT provide significant implications for the implementation of mitigation policies for regional to global ecosystems with substantial young plantations. Moreover, the MDF framework we developed has the potential to facilitate future model intercomparisons, benchmarking, and optimization at large scales, as well as to effectively quantify and then reduce the uncertainty in ecosystem C sequestration by estimating MTT in the disequilibrium state with long-term and multi-source observations.

ACKNOWLEDGEMENTS

We are grateful to Jianyang Xia for helpful comments on the manuscript. This study was supported by the National Key Research and Development Program of China (grant no. 2016YFC0500204), the Strategic Priority Research Program of the Chinese Academy of

Sciences (grant no. XDA19020301), and the National Natural Science Foundation of China (grant nos. 41571424 and 31700417). We thank the CERN staff for their dedication to observation and data processing.

ORCID

Rong Ge  <https://orcid.org/0000-0003-1846-7576>

Guoyi Zhou  <https://orcid.org/0000-0002-5667-7411>

Qibin Zhang  <https://orcid.org/0000-0001-5079-9402>

Weijun Shen  <https://orcid.org/0000-0001-7574-8839>

REFERENCES

- Ahlström, A., Schurgers, G., Armeth, A., & Smith, B. (2012). Robustness and uncertainty in terrestrial ecosystem carbon response to CMIP5 climate change projections. *Environmental Research Letters*, 7(4), 044008.
- Anav, A., Friedlingstein, P., Kidston, M., Bopp, L., Ciais, P., Cox, P., ... Zhu, Z. (2013). Evaluating the land and ocean components of the global carbon cycle in the CMIP5 Earth System Models. *Journal of Climate*, 26(18), 6801–6843.
- Barrett, D. J. (2002). Steady state turnover time of carbon in the Australian terrestrial biosphere. *Global Biogeochemical Cycles*, 16(4), 55–1–55–21.
- Bellassen, V., Delbart, N., Le Maire, G., Luysaert, S., Ciais, P., & Viovy, N. (2011). Potential knowledge gain in large-scale simulations of forest carbon fluxes from remotely sensed biomass and height. *Forest ecology and management*, 261(3), 515–530.
- Bloom, A. A., Exbrayat, J. F., Ir, V. D. V., Feng, L., & Williams, M. (2016). The decadal state of the terrestrial carbon cycle: Global retrievals of terrestrial carbon allocation, pools, and residence times. *Proceedings of the National Academy of Sciences*, 113(5), 1285–1290.
- Bloom, A. A., & Williams, M. (2015). Constraining ecosystem carbon dynamics in a data-limited world: Integrating ecological "common sense" in a model-data fusion framework. *Biogeosciences*, 12(5), 1299–1315.
- Bolin, B., & Rodhe, H. (1973). A note on the concepts of age distribution and transit time in natural reservoirs. *Tellus*, 25(1), 58–62.
- Carvalho, N., Forkel, M., Khomik, M., Bellarby, J., Jung, M., Migliavacca, M., ... Weber, U. (2014). Global covariation of carbon turnover times with climate in terrestrial ecosystems. *Nature*, 514(7521), 213–217.
- Carvalho, N., Reichstein, M., Ciais, P., Collatz, G. J., Mahecha, M. D., Montagnani, L., ... Seixas, J. (2010). Identification of vegetation and soil carbon pools out of equilibrium in a process model via eddy covariance and biometric constraints. *Global Change Biology*, 16(10), 2813–2829.
- Carvalho, N., Reichstein, M., Seixas, J., Collatz, G. J., Pereira, J. S., Berbigier, P., ... Rambal, S. (2008). Implications of the carbon cycle steady state assumption for biogeochemical modeling performance and inverse parameter retrieval. *Global Biogeochemical Cycles*, 22(2), 1081–1085.
- Chen, S., Huang, Y., Zou, J., & Shi, Y. (2013). Mean residence time of global topsoil organic carbon depends on temperature, precipitation and soil nitrogen. *Global and Planetary Change*, 100, 99–108.
- Chen, G. S., Yang, Y. S., Ping-Ping, L., & Zhang, Y. P. (2008). Regional patterns of soil respiration in china's forests. *Acta Ecologica Sinica*, 28(4), 1748–1761.
- De Kauwe, M. G., Medlyn, B. E., Zaehle, S., Walker, A. P., Dietze, M. C., Wang, Y. P., ... Wärlind, D. (2014). Where does the carbon go? A model-data intercomparison of vegetation carbon allocation and turnover processes at two temperate forest free-air CO₂ enrichment sites. *New Phytologist*, 203(3), 883–899.
- Erb, K. H., Fetzl, T., Plutzer, C., Kastner, T., Lauk, C., Mayer, A., ... Haberl, H. (2016). Biomass turnover time in terrestrial ecosystems halved by land use. *Nature Geoscience*, 9(9), 674–678.
- Exbrayat, J. F., Pitman, A. J., & Abramowitz, G. (2014). Response of microbial decomposition to spin-up explains CMIP5 soil carbon range until 2100. *Geoscientific Model Development*, 7(6), 2683–2692.
- Fox, A., Williams, M., Richardson, A. D., Cameron, D., Gove, J. H., Quaife, T., ... Van Wijk, M. T. (2009). The REFLEX project: Comparing different algorithms and implementations for the inversion of a terrestrial ecosystem model against eddy covariance data. *Agricultural and Forest Meteorology*, 149(10), 1597–1615.
- Frank, D. A., Pontes, A. W., & McFarlane, K. J. (2012). Controls on soil organic carbon stocks and turnover among North American ecosystems. *Ecosystems*, 15(4), 604–615.
- Friedlingstein, P., Cox, P., Betts, R., Bopp, L., von Bloh, W., Brovkin, V., ... Bala, G. (2006). Climate-carbon cycle feedback analysis: Results from the C⁴MIP model intercomparison. *Journal of Climate*, 19(14), 3337–3353.
- Friend, A. D., Lucht, W., Rademacher, T. T., Keribin, R., Betts, R., Cadule, P., ... Ito, A. (2014). Carbon residence time dominates uncertainty in terrestrial vegetation responses to future climate and atmospheric CO₂. *Proceedings of the National Academy of Sciences of the United States of America*, 111(9), 3280–3285.
- Galbraith, D., Malhi, Y., Affum-Baffoe, K., Castanho, A. D., Doughty, C. E., Fisher, R. A., ... Sonké, B. (2013). Residence times of woody biomass in tropical forests. *Plant Ecology & Diversity*, 6(1), 139–157.
- Gill, R. A., & Jackson, R. B. (2000). Global patterns of root turnover for terrestrial ecosystems. *The New Phytologist*, 147(1), 13–31.
- Goulden, M. L., McMillan, A. M. S., Winston, G. C., Rocha, A. V., Manies, K. L., Harden, J. W., & Bond-Lamberty, B. P. (2011). Patterns of NPP, GPP, respiration, and NEP during boreal forest succession. *Global Change Biology*, 17(2), 855–871.
- Hararu, O., Smith, M. J., & Luo, Y. (2015). Microbial models with data-driven parameters predict stronger soil carbon responses to climate change. *Global Change Biology*, 21(6), 2439–2453.
- He, Y., Trumbore, S. E., Torn, M. S., Harden, J. W., Vaughn, L. J., Allison, S. D., & Randerson, J. T. (2016). Radiocarbon constraints imply reduced carbon uptake by soils during the 21st century. *Science*, 353(6306), 1419–1424.
- Huang, S., Arain, M. A., Arora, V. K., Yuan, F., Brodeur, J., & Peichl, M. (2011). Analysis of nitrogen controls on carbon and water exchanges in a conifer forest using the CLASS-CTEMN+ model. *Ecological Modelling*, 222(20–22), 3743–3760.
- IPCC. (2013). Climate change 2013: The physical science basis. In T. F. Stocker, D. Qin, G.-K. Plattner, M. Tignor, S. K. Allen, J. Boschung ... P. M. Midgley (Eds.), *Contribution of working group 1 to the fifth assessment report of the intergovernmental panel on climate change* (1535 pp.). Cambridge, UK: Cambridge University Press.
- Ji, J. J. (1995). A climate-vegetation interaction model: Simulating physical and biological processes at the surface. *Journal of Biogeography*, 22, 2063–2069. <https://doi.org/10.2307/2845941>
- Karhu, K., Fritze, H., Tuomi, M., Vanhala, P., Spetz, P., Kitunen, V., & Liski, J. (2010). Temperature sensitivity of organic matter decomposition in two boreal forest soil profiles. *Soil Biology and Biochemistry*, 42(1), 72–82.
- Koven, C. D., Chambers, J. Q., Georgiou, K., Knox, R., Negron-Juarez, R., Riley, W. J., ... Jones, C. D. (2015). Controls on terrestrial carbon feedbacks by productivity versus turnover in the CMIP5 Earth System Models. *Biogeosciences*, 12(17), 5211–5228.
- Koven, C. D., Hugelius, G., Lawrence, D. M., & Wieder, W. R. (2017). Higher climatological temperature sensitivity of soil carbon in cold than warm climates. *Nature Climate Change*, 7(11), 817–822.
- Law, B. E., Thornton, P. E., Irvine, J., Anthoni, P. M., & Van, T. S. (2001). Carbon storage and fluxes in ponderosa pine forests at different developmental stages. *Global Change Biology*, 7(7), 755–777.

- Le Quéré, C., Andrew, R. M., Friedlingstein, P., Sitch, S., Pongratz, J., Manning, A. C., ... Boden, T. A. (2018). Global carbon budget 2017. *Earth System Science Data*, 10(1), 405–448.
- Le Toan, T., Quegan, S., Davidson, M. W. J., Balzter, H., Paillou, P., Pappathanassiou, K., ... Ulander, L. (2011). The BIOMASS mission: Mapping global forest biomass to better understand the terrestrial carbon cycle. *Remote Sensing of Environment*, 115(11), 2850–2860.
- Li, C., He, H. L., Liu, M., Su, W., Fu, Y. L., Zhang, L. M., ... Yu, G. R. (2008). The design and application of CO₂ flux data processing system at ChinaFLUX. *Geo-Information Science*, 10(5), 557–565.
- Li, X. J., Zhou, T., & He, X. Z. (2009). Carbon sink of forest ecosystem driven by NPP increasing in China. *Journal of Natural Resources*, 24(3), 491–497.
- Liu, Y., He, N., Zhu, J., Xu, L., Yu, G., Niu, S., ... Wen, X. (2017). Regional variation in the temperature sensitivity of soil organic matter decomposition in China's forests and grasslands. *Global Change Biology*, 23(8), 3393–3402.
- Liu, H., Tang, L. Q., Hu, B., Liu, G. R., Wang, Y. S., Bai, F., ... Zhu, Y. J. (2017). Photosynthetically active radiation dataset in Chinese Ecosystem Research Network (2005–2015). *China Scientific Data*, 2(1), 1–10.
- Lugo, A. E., & Brown, S. (1986). Steady state terrestrial ecosystems and the global carbon cycle. *Vegetatio*, 68(2), 83–90.
- Luo, Y., Shi, Z., Lu, X., Xia, J., Liang, J., Jiang, J., ... Chen, B. (2017). Transient dynamics of terrestrial carbon storage: Mathematical foundation and numeric examples. *Biogeosciences*, 14(1), 145–161.
- Luo, Y., & Weng, E. (2011). Dynamic disequilibrium of the terrestrial carbon cycle under global change. *Trends in Ecology & Evolution*, 26(2), 96–104.
- Luo, Y., White, L. W., Canadell, J. G., DeLucia, E. H., Ellsworth, D. S., Finzi, A., ... Schlesinger, W. H. (2003). Sustainability of terrestrial carbon sequestration: A case study in Duke Forest with inversion approach. *Global biogeochemical cycles*, 17(1), 1021. <https://doi.org/10.1029/2002GB001923>
- Luyssaert, S., Schulze, E. D., Börner, A., Knohl, A., Hessenmöller, D., Law, B. E., ... Grace, J. (2008). Old-growth forests as global carbon sinks. *Nature*, 455(7210), 213–215.
- Mantgem, P. J. V., Stephenson, N. L., Byrne, J. C., Daniels, L. D., Franklin, J. F., Fulé, P. Z., ... Veblen, T. T. (2009). Widespread increase of tree mortality rates in the western United States. *Science*, 323(5913), 521–524.
- Manzoni, S., & Porporato, A. (2009). Soil carbon and nitrogen mineralization: Theory and models across scales. *Soil Biology and Biochemistry*, 41(7), 1355–1379.
- Medlyn, B. E., Zaehle, S., De Kauwe, M. G., Walker, A. P., Dietze, M. C., Hanson, P. J., ... Prentice, I. C. (2015). Using ecosystem experiments to improve vegetation models. *Nature Climate Change*, 5(6), 528–534.
- Mi, N., Yu, G., Wang, P., Wen, X., & Sun, X. (2006). A preliminary study for spatial representiveness of flux observation at ChinaFLUX sites. *Science in China Series D Earth Sciences*, 49(2), 24–35.
- Morales, P., Sykes, M. T., Prentice, I. C., Smith, P., Smith, B., Bugmann, H., ... Sánchez, A. (2005). Comparing and evaluating process-based ecosystem model predictions of carbon and water fluxes in major European forest biomes. *Global Change Biology*, 11(12), 2211–2233.
- Negrón-Juárez, R. I., Koven, C. D., Riley, W. J., Knox, R. G., & Chambers, J. Q. (2015). Observed allocations of productivity and biomass, and turnover times in tropical forests are not accurately represented in cmip5 earth system models. *Environmental Research Letters*, 10(6), 064017.
- Odum, E. P. (1966). The strategy of ecosystem development. *Science*, 164, 262–270.
- Pan, Y. D., Birdsey, R. A., Fang, J. Y., Houghton, R., Kauppi, P. E., Kurz, W. A., ... Hayes, D. (2011). A large and persistent carbon sink in the world's forests. *Science*, 333, 988–993.
- Piao, S., Fang, J., Ciais, P., Peylin, P., Huang, Y., Sitch, S., & Wang, T. (2009). The carbon balance of terrestrial ecosystems in China. *Nature*, 458(7241), 1009–1013.
- Piao, S., Luyssaert, S., Ciais, P., Janssens, I. A., Chen, A., Cao, C., ... Wang, S. (2010). Forest annual carbon cost: A global-scale analysis of autotrophic respiration. *Ecology*, 91(3), 652–661.
- Pietsch, S. A., & Hasenauer, H. (2006). Evaluating the self-initialization procedure for large-scale ecosystem models. *Global Change Biology*, 12(9), 1658–1669.
- Post, W. M., Pastor, J., Zinke, P. J., & Stangenberger, A. G. (1985). Global patterns of soil nitrogen storage. *Nature*, 317(6038), 613–616. <https://doi.org/10.1038/317613a0>
- Reich, P. B., Luo, Y. J., Bradford, J. B., Poorter, H., Perry, C. H., & Oleksyn, J. (2014). Temperature drives global patterns in forest biomass distribution in leaves, stems, and roots. *Proceedings of the National Academy of Sciences of the United States of America*, 111(38), 13721–13727.
- Richardson, A. D., Williams, M., Hollinger, D. Y., Moore, D. J., Dail, D. B., Davidson, E. A., ... Rodrigues, C. (2010). Estimating parameters of a forest ecosystem model with measurements of stocks and fluxes as joint constraints. *Oecologia*, 164(1), 25–40.
- Rodhe, H. (1978). Budgets and turn-over times of atmospheric sulfur compounds. *Sulfur in the Atmosphere*, 12(1–3), 671–680.
- Safta, C., Ricciuto, D. M., Sargsyan, K., Debusschere, B., Najm, H. N., Williams, M., & Thornton, P. E. (2015). Global sensitivity analysis, probabilistic calibration, and predictive assessment for the data assimilation linked ecosystem carbon model. *Geoscientific Model Development Discussions*, 8(7), 6893–6948.
- Sanderman, J., Amundson, R. G., & Baldocchi, D. D. (2003). Application of eddy covariance measurements to the temperature dependence of soil organic matter mean residence time. *Global Biogeochemical Cycles*, 17(2), 30–31.
- Schwartz, S. E. (1979). Residence times in reservoirs under non-steady-state conditions: Application to atmospheric SO₂ and aerosol sulfate. *Tellus*, 31(6), 530–547.
- Sierra, C. A., Müller, M., Metzler, H., Manzoni, S., & Trumbore, S. E. (2017). The middle of ages, turnover, transit, and residence times in the carbon cycle. *Global Change Biology*, 23(5), 1763–1773.
- Sitch, S., Smith, B., Prentice, I. C., Arneth, A., Bondeau, A., Cramer, W., ... Thonicke, K. (2003). Evaluation of ecosystem dynamics, plant geography and terrestrial carbon cycling in the LPJ dynamic global vegetation model. *Global Change Biology*, 9(2), 161–185.
- Smallman, T. L., Exbrayat, J. F., Mencuccini, M., Bloom, A. A., & Williams, M. (2017). Assimilation of repeated woody biomass observations constrains decadal ecosystem carbon cycle uncertainty in aggrading forests. *Journal of Geophysical Research: Biogeosciences*, 122(3), 528–545.
- Strand, A. E., Pritchard, S. G., McCormack, M. L., Davis, M. A., & Oren, R. (2008). Irreconcilable differences: Fine-root life spans and soil carbon persistence. *Science*, 319(5862), 456–458.
- Taylor, K. E., Stouffer, R. J., & Meehl, G. A. (2012). An overview of cmip5 and the experiment design. *Bulletin of the American Meteorological Society*, 93(4), 485–498.
- Thornton, P. E., & Rosenbloom, N. A. (2005). Ecosystem model spin-up: Estimating steady state conditions in a coupled terrestrial carbon and nitrogen cycle model. *Ecological Modelling*, 189(1–2), 25–48.
- Turner, M., Beer, C., Carvalhais, N., Forkel, M., Santoro, M., Tum, M., & Schimmlius, C. (2016). Large-scale variation in boreal and temperate forest carbon turnover rate is related to climate. *Geophysical Research Letters*, 43(9), 4576–4585.
- Turner, M., Beer, C., Ciais, P., Friend, A. D., Ito, A., Kleidon, A., ... Tum, M. (2017). Evaluation of climate-related carbon turnover processes in global vegetation models for boreal and temperate forests. *Global Change Biology*, 23(8), 3076–3091.
- Todd-Brown, K. E. O., Randerson, J. T., Post, W. M., Hoffman, F. M., Tarnocai, C., Schuur, E. A. G., & Allison, S. D. (2013). Causes of variation in soil carbon simulations from CMIP5 Earth system models and comparison with observations. *Biogeosciences*, 10(13), 1717–1736.

- Trumbore, S. (2006). Carbon respired by terrestrial ecosystems—recent progress and challenges. *Global Change Biology*, 12(2), 141–153.
- Wang, W., Dungan, J., Hashimoto, H., Michaelis, A. R., Milesi, C., Ichii, K., & Nemani, R. R. (2011). Diagnosing and assessing uncertainties of the carbon cycle in terrestrial ecosystem models from a multi-model ensemble experiment. *Global Change Biology*, 17(3), 1350–1366.
- Wang, J., Sun, J., b, J., He, N., Li, M., & Niu, S. (2018). Soil and vegetation carbon turnover times from tropical to boreal forests. *Functional Ecology*, 32(1), 71–82.
- Williams, M., Schwarz, P. A., Law, B. E., Irvine, J., & Kurpius, M. R. (2005). An improved analysis of forest carbon dynamics using data assimilation. *Global Change Biology*, 11(1), 89–105.
- Wutzler, T., & Reichstein, M. (2007). Soils apart from equilibrium? consequences for soil carbon balance modelling. *Biogeosciences*, 4, 125–136.
- Xia, J., Chen, Y., Liang, S., Liu, D., & Yuan, W. (2015). Global simulations of carbon allocation coefficients for deciduous vegetation types. *Tellus Series B-chemical & Physical Meteorology*, 67(2), 28016.
- Xia, J., Luo, Y., Wang, Y. P., & Hararuk, O. (2013). Traceable components of terrestrial carbon storage capacity in biogeochemical models. *Global Change Biology*, 19(7), 2104–2116.
- Xia, J. Y., Luo, Y. Q., Wang, Y. P., Weng, E. S., & Hararuk, O. (2012). A semi-analytical solution to accelerate spin-up of a coupled carbon and nitrogen land model to steady state. *Geoscientific Model Development*, 5(5), 1259–1271.
- Xu, T., White, L., Hui, D., & Luo, Y. (2006). Probabilistic inversion of a terrestrial ecosystem model: Analysis of uncertainty in parameter estimation and model prediction. *Global Biogeochemical Cycles*, 20(2), GB2007. <https://doi.org/10.1029/2005GB002468>
- Xue, B. L., Guo, Q., Hu, T., Xiao, J., Yang, Y., Wang, G., ... Zhao, X. (2017). Global patterns of woody residence time and its influence on model simulation of aboveground biomass. *Global Biogeochemical Cycles*, 31(5), 821–835.
- Yan, Y., Luo, Y., Zhou, X., & Chen, J. (2014). Sources of variation in simulated ecosystem carbon storage capacity from the 5th Climate Model Intercomparison Project (CMIP5). *Tellus B: Chemical and Physical Meteorology*, 66(1), 22568.
- Yan, Y., Zhou, X., Jiang, L., & Luo, Y. (2017). Effects of carbon turnover time on terrestrial ecosystem carbon storage. *Biogeosciences*, 14(23), 5441.
- Yu, G., Chen, Z., Piao, S., Peng, C., Ciais, P., Wang, Q., ... Zhu, X. (2014). High carbon dioxide uptake by subtropical forest ecosystems in the East Asian monsoon region. *Proceedings of the National Academy of Sciences*, 111(13), 4910–4915.
- Zaehle, S., Sitch, S., Prentice, I. C., Liski, J., Cramer, W., Erhard, M., ... Smith, B. (2006). The importance of age-related decline in forest NPP for modeling regional carbon balances. *Ecological Applications*, 16(4), 1555–1574.
- Zhang, C., Ju, W., Chen, J. M., Li, D., Wang, X., Fan, W., ... Zan, M. (2014). Mapping forest stand age in China using remotely sensed forest height and observation data. *Journal of Geophysical Research: Biogeosciences*, 119(6), 1163–1179.
- Zhang, L., Luo, Y., Yu, G., & Zhang, L. (2010). Estimated carbon residence times in three forest ecosystems of eastern China: Applications of probabilistic inversion. *Journal of Geophysical Research: Biogeosciences*, 115(G1), 137–147.
- Zhang, X., & Wu, K. (2001). Fine-root production and turnover for forest ecosystems. *Scientia Sinicae*, 37(3), 126–138.
- Zhao, X., Guan, D., Wu, J., Jin, C. J., & Han, S. J. (2005). Distribution of footprint and flux source area of the mixed forest of broad-leaved and Korean pine in Changbai Mountain. *Journal of Beijing Forest University*, 27(3), 17–23.
- Zheng, Z. M., Yu, G. R., Sun, X. M., Li, S. G., Wang, Y. S., Wang, Y. H., ... Wang, Q. F. (2010). Spatio-temporal variability of soil respiration of forest ecosystems in China: Influencing factors and evaluation model. *Environmental Management*, 46(4), 633–642.
- Zhou, G., Liu, S., Li, Z., Zhang, D., Tang, X., Zhou, C., ... Mo, J. (2006). Old-growth forests can accumulate carbon in soils. *Science*, 314(5804), 1417–1417.
- Zhou, T., & Luo, Y. (2008). Spatial patterns of ecosystem carbon residence time and NPP-driven carbon uptake in the conterminous United States. *Global Biogeochemical Cycles*, 22(3), 3411–3434.
- Zhou, G., Peng, C., Li, Y., Liu, S., Zhang, Q., Tang, X., ... Chu, G. (2013). A climate change-induced threat to the ecological resilience of a subtropical monsoon evergreen broad-leaved forest in Southern China. *Global Change Biology*, 19(4), 1197–1210.
- Zhou, T., Shi, P., Hui, D., & Luo, Y. (2009). Spatial patterns in temperature sensitivity of soil respiration in china: estimation with inverse modeling. *Science in China*, 52(10), 982–989.
- Zhou, T., Shi, P., Jia, G., Li, X., & Luo, Y. (2010). Spatial patterns of ecosystem carbon residence time in Chinese forests. *Science China Earth Sciences*, 53(8), 1229–1240.
- Zhou, T., Shi, P., Jia, G., & Luo, Y. (2013). Nonsteady state carbon sequestration in forest ecosystems of china estimated by data assimilation. *Journal of Geophysical Research Biogeosciences*, 118(4), 1369–1384.
- Zhu, G., Ju, W., Chen, J. M., Gong, P., Xing, B., & Zhu, J. (2012). Foliage clumping index over China's landmass retrieved from the MODIS BRDF parameters product. *IEEE Transactions on Geoscience and Remote Sensing*, 50(6), 2122–2137.
- Zobitz, J., Desai, A., Moore, D., & Chadwick, M. (2011). A primer for data assimilation with ecological models using Markov Chain Monte Carlo (MCMC). *Oecologia*, 167(3), 599–611.

SUPPORTING INFORMATION

Additional supporting information may be found online in the Supporting Information section at the end of the article.

How to cite this article: Ge R, He H, Ren X, et al. Underestimated ecosystem carbon turnover time and sequestration under the steady state assumption: A perspective from long-term data assimilation. *Glob Change Biol*. 2019;25:938–953. <https://doi.org/10.1111/gcb.14547>